Characterization and Development of Osmotolerant Caldicellulosiruptor Strains Targeting Enhanced Hydrogen Production from Lignocellulosic Hydrolysates

Eoin Byrne
Lund University: Lunds Universitet
Johanna Björkmalm
RISE Research Institutes of Sweden AB
James Bostick
Lunds Universitet
Krishnan Sreenivas
Lunds Universitet
Karin Willquist
RISE Research Institutes of Sweden AB
Ed Van Niel (ed.van_niel@tmb.lth.se)
Lund University https://orcid.org/0000-0003-2103-6013

Research

Keywords: Osmolarity, Caldicellulosiruptor, biohydrogen, kinetic model, adaptive laboratory evolution

Posted Date: December 7th, 2020

DOI: https://doi.org/10.21203/rs.3.rs-118276/v1

Characterization and development of osmotolerant *Caldicellulosiruptor* strains targeting enhanced hydrogen production from lignocellulosic hydrolysates

Eoin Byrne[1], Johanna Björkmalm[1,2], James P. Bostick[1], Krishnan Sreenivas[1], Karin Willquist[2], Ed W.J. van Niel[1]

[1] Division of Applied Microbiology, Lund University, PO Box 124, 221 00 Lund, Sweden
[2] RISE, Ideon Science Park, Building Beta 2 3v Scheelevägen 17, SE-22370 Lund

Keywords
Osmolarity, *Caldicellulosiruptor*, biohydrogen, kinetic model, adaptive laboratory evolution

Abstract

Background

The members of the genus *Caldicellulosiruptor* have the potential for future integration into a biorefinery system due to their capacity to generate hydrogen close to the theoretical limit of 4 mol H_2 /mol hexose, use a wide range of sugars and can grow on numerous lignocellulose hydrolysates. However, members of this genus are unable to survive in high osmolarity conditions, limiting their ability to grow on more concentrated hydrolysates, thus impeding their industrial applicability. In this study five members of this genus, *C. owensensis*, C. *kronotskyensis*, *C. bescii, C. acetigenus* and *C. kristjanssonii*, were developed to tolerate higher osmolarities through an adaptive laboratory evolution (ALE) process. The developed strain *C. owensensis* CO80 was further studied accompanied by the development of a kinetic model based on Monod kinetics.

Results

Osmotolerant strains of *Caldicellulosiruptor* were obtained with *C. owensensis* adapted to grow up to 80 g/l glucose; other strains in particular C. *kristjanssonii* demonstrated a greater restriction to adaptation. *C. owensensis* CO80 was further studied and demonstrated the ability to grow in glucose concentrations up to 80 g/l glucose but with reduced volumetric hydrogen productivities (Q_{H2}) and incomplete sugar conversion at elevated glucose concentrations. In addition, the carbon yield decreased with elevated concentrations of glucose. The ability of *C. owensensis* CO80 to grow in high glucose concentrations was further described with a kinetic growth model, which revealed that the critical osmolarity of the cells increased fourfold when cultivated at higher osmolarity. When co-cultured with the osmotolerant strain *C. saccharolyticus* G5 at a hydraulic retention time (HRT) of 20h, *C. owensensis* constituted only 0.09-1.58% of the population in suspension.

Conclusions

The adaptation of members of the *Caldicellulosiruptor* genus to higher osmolarity established that the ability to develop improved strains via ALE is species dependent, with *C. owensensis* adapted to grow on 80 g/l, whereas *C. kristjanssonii* could only be adapted to 30 g/l glucose. Although, *C. owensensis* CO80 was adapted to a higher osmolarity medium, the strain demonstrated reduced Q_{H2} with elevated glucose concentrations. This would indicate that while ALE permits adaptation to elevated osmolarities, this approach does not result in improved fermentation performances at these higher osmolarities. Moreover, the observation that planktonic culture of CO80 was outcompeted by an osmotolerant strain of *C. saccharolyticus,* when co-cultivated in continuous mode, indicates that the robustness of strain CO80 should be improved for industrial application.

Background

The current reliance on fossil fuels as the main source of global energy production is not sustainable.. Biofuels derived from renewable sources are an extensively researched alternative for the production of energy, however, it is of great importance these fuels do not compete with food production in terms of land usage (Sims et al., 2008). Within the European Union, current legislation restricts dedicated biofuel production to 7% of total land use (European Parliament and Council, 2015). Lignocellulose is a potential substrate for biofuel production due to its wide availability with 1-5 billion tonnes yielded annually (Claassen et al., 1999). Currently, over 40 million tonnes of this material is generated as a by-product of agriculture and forestry (Sanderson, 2011), and is ideally suited for biofuel production as lignocellulose obtained from waste streams does not affect land usage or food production.

Biologically derived hydrogen (biohydrogen) has the potential to be an alternative energy carrier as it can be produced from renewable sources such as lignocellulose and only generates water vapor as a by-product when used as a fuel (Azwar et al., 2014). *Caldicellulosiruptor* is a genus of thermophilic hydrogen producing bacteria capable of yielding hydrogen close to the maximum stoichiometric yield of 4 mol H_2/mol hexose (Rainey et al., 1994; Schleifer, 2009). Notably, most members of this genus can metabolize a wide range of carbon sources including an array of mono-, oligo- and polysaccharides (Schleifer, 2009). Species such as *C. saccharolyticus* and *C. owensensis* display the capacity to simultaneously consume hexoses and pentoses without catabolite repression and therefore is beneficial to an industrial process as both the cellulose and hemicellulose fractions of lignocellulose can be consumed together (Björkmalm et al., 2018; VanFossen et al., 2009; Zeidan & van Niel, 2010). Additionally, *Caldicellulosiruptor* has been previously utilized to generate hydrogen from a variety of lignocellulosic material (Byrne et al., 2018; de Vrije et al., 2009; Pawar et al., 2013).

Although a promising candidate for industrial biohydrogen production, *Caldicellulosiruptor* experiences several key limitations including the ability to grow in high osmotic conditions (Byrne et al., 2018; Ljunggren et al., 2011; Pawar et al., 2013). In its natural environment *Caldicellulosiruptor* does not experience a high degree of osmotic stress and has thus adapted to low osmolarities, maximally of 0.4 to 0.425 Osmol/L, with a critical osmolarity of 0.27 to 0.29 Osmol/L. This osmo-sensitivity limits the industrial potential of *Caldicellulosiruptor* as it precludes cultivation in concentrated lignocellulose hydrolysates. Concentrated hydrolysates are essential for environmentally efficient production of thermophilic H_2 as higher substrate concentrations reduce the requirement for water addition and energy input for heating (Byrne et al., 2018; Foglia et al., 2010; Ljunggren & Zacchi, 2010).

Mathematical modeling is a powerful tool to assess how the key physical and biological phenomena in a process function. Inhibition arising from osmosensitivity can be one such phenomenon and is further addressed in this paper. This modeling of quantitative description of substrate inhibition and inhibition due to a high degree of osmotic stress have previously been studied using different types of growth kinetic equations (Azimian et al., 2019; Ciranna et al., 2014; Dötsch et al., 2008; van Niel et al., 2003). A non-competitive equation is commonly used to describe growth inhibition due to substrate or soluble end products (Ciranna et al., 2014; van Niel et al., 2003).

One way to improve osmotolerance in microorganisms is through targeting genes involved in responses to increased osmotic pressure through metabolic engineering and has become an intensive research approach (Lv et al 2020). Recently, *C. bescii* was investigated to identify its response mechanism to higher osmolarities, which then can be targeted by directed engineering (Sander et al., 2020). Alternatively, when genetic engineering tools are missing strain improvement can be accomplished through a process known as adaptive laboratory evolution (ALE). In this process an organism is repeatedly sub-cultivated under defined conditions enabling a controlled adaptation to these conditions and hence a favorable phenotype change can develop (Dragosits & Mattanovich, 2013). We have applied this successively with *C. saccharolyticus* (Pawar 2014), and here we describe the development of several osmotolerant strains of other *Caldicellulosiruptor* species, i.e., *C. owensensis, C. kronotsyensis, C. bescii, C. acetigenus* and *C. kristjanssonii* through sequential ALE at incrementally increasing glucose concentrations. The adapted osmotolerant strain *C. owensensis* (CO80) was cultivated in controlled batch and exposed to a high concentration of glucose, up to 80 g/L. To quantify the success of strain development, this process was modelled using a growth kinetic equation based on Monod with a set of inhibition equations. Finally, *C. owensensis* CO80 was further analyzed in co-cultures with the osmotolerant strain G5 of *C.*

saccharolyticus (Pawar 2014), on defined media and lignocellulosic hydrolysate of which the data have been published elsewhere (Byrne et al. (2018).

Results

Strain development

To assess the ability of different strains of the *Caldicellulosiruptor* genus to adapt to higher osmolarity and to select an osmotolerant strain for further development, ALE was undertaken on five species of *Caldicellulosiruptor*. The respective increase in viability at higher osmolarity was determined during sequential batches, whereby increased sugar concentration was used as a selective pressure.

The ALE design replicated a previous study that achieved the selection of a *C. saccharolyticus* strain with the capacity to grow on 100 g/L glucose (Pawar, 2014). Out of the five selected strains, only *C. owensensis* was successfully adapted to grow on a glucose concentration of 80 g/L (Figure 1) over the course of approximately 250 generations. The adaptation of *C. kronotskyensis* demonstrated viability in solutions up to 60 g/L glucose but at 70 g/L it did not reach the threshold value of OD_{620} 0.4 and therefore was not selected for further analysis. In contrast, the adaptation strategy of *C. kristjanssonii, C. bescii* and *C. acetigenus* was quite restrictive. Even with repeated cultivation at lower sugar concentrations a loss of viability occurred. *C. kristjanssonii* was particularly sensitive to adaptation and exhibited poor viability in glucose concentrations as low as 20 g/L. Overall, *C. owensensis* had a greater ability to adapt to higher osmolarity medium than any other strain. Adaptation of *C. owensensis* to 100 g/L glucose was attempted, however, strains adapted to 90 and 100 g/L displayed poor growth and a loss of viability after several rounds of cultivation. Therefore, the *C. owensensis* strain adapted to 80 g/L glucose (CO80) was selected for further analysis.

Adaptation of bacterial cells to higher osmolalities is usually related to intracellular accumulation of compatible solutes and therefore a focused bioinformatics study was performed (Kempf & Bremer, 1998). However, similar to *C. saccharolyticus* (Willquist et al., 2009), *C. owensensis* lacks key metabolic pathways for the synthesis of compatible solutes for high osmotic conditions. *C. owensensis* lacks synthetic pathways for the osmoprotectants glycine betaine, ectoine and trehalose. *C. owensensis* also lacks pathways associated with the synthesis of compatible solutes in thermophiles such as the di-myo-inositol phosphate pathway (Gonçalves et al., 2012; Martins & Santos, 1995) and the synthesis pathway for 2-O-(β)-mannosylglycerate as found in *Thermus thermophilus* (Nunes et al., 1995). In addition, no homology between the *C. owensensis* genome and 2-(O-β-d-mannosyl)-di-myo-inositol-1,3′-phosphate synthase (TM0359) in *Thermotoga maritima* (Rodrigues et al., 2009) could be found. However, *C. owensensis* can produce glutamate and has the full synthetic pathway of proline.

Quantitative analysis of CO80 growth at higher sugar concentrations

C. owensensis CO80 was successfully cultivated on 10, 30 and 80 g/L using a controlled batch reactor. The trends of sugar consumption, growth and product formation in these cultures on these different sugar concentrations were monitored (Figures 2-4).

The behavior of strain CO80 at increasing glucose concentrations was quantified using dynamic simulations. In these simulations, the model and parameters derived from the wild-type strain of *C. saccharolyticus* were used as a benchmark (Ljunggren et al., 2011). However, this model was not able to describe the experimental data. One reason for this is that the benchmark value of the parameter OSM_{crit} taken from Ljunggren et al. (2011) was set too low for the

higher glucose concentrations. In addition, the benchmark values for parameters of the maximum specific growth rate (μ_{max}), affinity constant for glucose (K_s) and the rate of death (r_{cd}) required alteration since the growth was slower and the cell death rate was higher than predicted by the original model.

Table 1. Parameters calibrated to experimental data of *C. owensensis* cultures in comparison to the benchmark parameter values of *C. saccharolyticus* cultures from Ljunggren et al (2011).

Parameter	Benchmark values Ljunggren et al. (2011)	10 g/L	30 g/L[1]	30 g/L[2]	80 g/L
μ_{max} (h^{-1})	0.28	0.33 ± 0	0.31 ± 0.082	0.31 ± 0.082	0.29 ± 0.02
K_S (mol/L)	$4.8 \cdot 10^{-5}$	$4.8 \cdot 10^{-3}$	$9.8 \cdot 10^{-2} \pm 1.5 \cdot 10^{-4}$	$4.8 \cdot 10^{-5}$, [5]	0.49 ± 0.064
OSM_{crit} (mol/L)	0.28	0.23 ± 0.0002	0.39 ± 0.002	0.39 ± 0.002	0.78 ± 0.024
r_{cd} (h^{-1})	0.014	0.031 ± 0.0001	0.031 ± 0.0065	0.020 ± 0.00015	0.031[3]
$Y_{S,H2}$ (mol/mol)	4.77	3.5 ± 0.38	3.5 ± 0.12	3.5 ± 0.12	2.56[3]
$Y_{S,X}$ (cmol/mol)	4.78	0.79[4]	0.80[4]	0.80[4]	0.72[3]
n_{H2}	4.5	5.37 ± 0.00005	5.37[3]	5.37[3]	4.5[5]
$n_{\mu.}$	4.68	4.68[5]	4.68[5]	4.68[5]	4.68[5]

Confidence interval 95% is given for those parameters which have been fitted numerically.
[1]First model for the 30 g/L cultures
[2]Second model for the 30 g/L cultures
[3]Graphically calibrated
[4]Calculated from experimental data
[5]Same value as in Ljunggren et al. (2011)

Therefore, the model was calibrated with all data from the duplicates or triplicates of the three batch experiments supplemented with 10 g/L, 30 g/L and

80 g/L glucose. The calibrated parameters μ_{max}, OSM_{crit} and K_S, together with additional parameters are summarized in Table 1. Comparison between the model and the experimental results are graphically shown in Figure 2-4.

The maximum hydrogen productivity from the experimental data was 10.55 ± 0.04, 11.45 ± 0.00 and 3.35 ± 0.00 mmol/L/h for 10, 30 and 80 g/L sugar, respectively. This observation at 10 and 30 g/L is comparable to 15 mmol/L/h described in wild-type *C. owensensis* grown on 10 g/L glucose supplemented with 1 g/L yeast extract (Zeidan & van Niel, 2010). The model underestimated the hydrogen productivity slightly in the case of 10 and 30 g/L but overestimated productivity compared to experimental data of 80 g/L cultures. Similar overestimation was observed with respect to the cell growth on 80 g/L. Nevertheless, the model was able to predict the experimental data adequately.

The accuracy of the model in describing experimental data was assessed (Table 2. The R^2 values describes how well the model could predict the trend over time and the curve slope values of the linear regression (i.e., k in $y = k \cdot x$) are indicating over- or underestimations. For a perfect fit they should both be 1. With respect to most variables, the prediction error was less than 30% indicating good accuracy. The model was also able to accurately predict the trend of the assessed variables with a R^2 value close to 1 in all cases. However, analysis revealed the overestimation of cell growth as well as acetate and lactate production of the cultures on 30 g/L glucose (Table 2).

Inhibition kinetics

The glucose concentration portrayed a linear relationship with the apparent half-saturation constant (K_S) and critical osmolarity (OSM_{crit}) (Figure 5). The apparent K_S increased with the elevating glucose concentration reaching a value four

241 **Table 2.** R^2 values and curve slope values to describe the fit between
242 average experimental data and simulated data from the models at the same
243 time points.
244

R^2 values/curve slope values (k)	**10 g/L**		**30 g/L**			**80 g/L**	
State variable	Model	K_S model	Model 1	Model 2	K_S model	Model	KS model
Glu	0.94/ 0.95	0.67/ 0.93	0.91/ 0.96	0.89/ 0.95	0.83/ 1.0	0.87/ 0.99	0.85/ 0.98
Biomass	0.82/ 0.96	0.77/ 1.0	0.50/ 6.0	0.28/ 6.8	0.82/ 4.2	0.96/ 0.43	0.94/ 0.43
Acetate	0.97/ 0.97	0.75/ 1.2	0.94/ 1.1	0.96/ 1.1	0.77/ 0.85	0.99/ 0.54	0.99/ 0.55
Lactate	0.95/ 1.4	0.60/ 1.5	0.97/ 2.0	0.92/ 2.1	0.83/ 1.4	0.97/ 0.54	0.98/ 0.54
H_2 accumulated	0.94/ 0.92	0.51/ 1.1	0.94/ 0.88	0.96/ 0.98	0.76/ 0.71	0.99/ 0.72	0.98/ 0.74
OSM	0.97/ 0.98	0.57/ 1.0	0.94/ 1.0	0.97/ 1.0	0.75/ 0.96	0.91/ 0.40*	0.92/ 0.40*

245 *The linear regression does not intersect (0,0).
246

247

248 orders of magnitude higher in the 80 g/L glucose culture. As Sivakumar et al.
249 (1994) demonstrated, extraordinarily high K_S values can be an indicator that the
250 growth kinetics applied is insufficient in describing the process due to substrate
251 inhibition, hence, an extended model was constructed. In the constructed "K_S-
252 model", the K_S in the original model (Eq 7 in Material and Methods) was
253 replaced with the equation from the linear regression in Figure 5:

$$\mu = \mu_{max} \cdot \frac{Glu}{Glu+(1.32 \cdot Glu-0.09)} \cdot I_{osm} \cdot I_{H_{2,aq}} \quad (1)$$

where μ is the specific growth rate (h^{-1}), μ_{max} the maximum specific growth rate (h^{-1}), Glu is the glucose concentration (mol/L), I_{osm} is the inhibition due to osmolarity and $I_{H2,aq}$ is the inhibition due to aqueous hydrogen concentration. The simulation using the "K_S-model" is illustrated in Figure 2-4 as a thin dashed line. The K_S-model was well able to describe the experimental data (Table 2) for 30 g/L and 80 g/L (Figure 3-4). However, for 10 g/L, the K_S-model could not sufficiently describe the data (Table 2). This may be due to the greater glucose consumption at 10 g/L compared to the higher concentrations, thereby altering the K_S-model equation to a greater extent than this model is dependent on the glucose concentration.

The increase of OSM_{crit} with the sugar concentration (Figure 5) indicates that strain CO80 adapts immediately when confronted with a raise in the osmolarity or sugar concentration in the medium. This behavior became more apparent when the inhibition kinetics of the fermentation was simulated in the different cases. The model describes two different types of inhibition, i.e., inhibition by osmolarity (I_{osm}) and dissolved hydrogen concentration ($I_{H2,aq}$) (Equation 6 and 7), which were simulated for all three glucose concentrations (Figure 6). A value around 1 means no inhibition and a lower value means that the process is inhibited. Figure 6 clearly shows that osmolarity is the crucial inhibition factor, i.e., an I_{osm} value <1. $I_{H2,aq}$ is of less importance as the simulated values were $0.98<I_{H2,aq}<1$, which means almost no inhibition. Although, the K_S model for 10 g/L gave values of $0.11<I_{H2,}aq<1$, this rather indicates that the model is not a good fit to the experimental data at this glucose concentration, which confirms what is depicted in Figure 2. Interestingly, the simulation of I_{osm} illustrates that although all fermentations was severely affected by osmolarity, strain CO80 grown on 80 g/L glucose reached complete inhibition after 80 h, whereas the cultivation on 10 g/L reached complete inhibition after 20 h, although the initial

osmolarity in this condition was lower. This indicates that although *C. owensensis* CO80 is adapted to higher osmolarities it does not manifest the phenotype unless it is stressed in an environment with a high osmolarity.

It should be noted that at high levels of sugar (80 g/L), significant browning of the media occurred likely due to the presence of Maillard products. This observation could not be quantified and described by the model.

Reproducibility of strain CO80

The model was also used to illustrate the reproducibility of growth of strain CO80 at increasing sugar concentrations. Three replicates were made for the 30 g/L experiments, as compared to two replicates for the 10 g/L and 80 g/L due to a high degree of variation in one of the replicates. Several attempts at inoculating strain CO80 to a culture medium containing 80 g/l glucose failed, as it did not grow when noticeable browning of the media due to Maillard reactions occurred. As illustrated in Figure 3, one of the three replicates (30b) from the 30 g/L experiments differed with respect to hydrogen productivity and accumulation but discrepancies could also be seen in the biomass growth. For this reason, a second model (Model 2) with a slight difference in parameter values (Table 1) was constructed for the 30 g/L experiments. However, both Model 1 and Model 2 resulted in low R^2 values and high curve slope values for the biomass (Table 2). One of the three replicates could be simulated with respect to OSM_{crit} and apparent saturation constant (K_S; Figure 3) whereas the other two could be fitted better with the model where the parameters were much closer to those of the 10 g/L culture. This result might indicate that the adaptation was incomplete, possibly due to the presence of subpopulations possessing different degrees of adaptation to higher osmolarity (Peabody et al., 2016).

Evaluation of strain CO80 in co-culture

The results of the batch cultivations indicated that *C. owensensis* CO80 was adapted to increased substrate concentrations but did not grow optimally at these conditions. A further attempt has been made to improve the performance of this strain by co-cultivation with the osmotolerant *C. saccharolyticus* strain G5 in defined media and wheat straw hydrolysate, of which the data were published elsewhere (Byrne et al., 2018). Overall, the co-cultures on wheat straw hydrolysate displayed better performance, such as higher Q_{H2} and sugar consumption rates, than on the defined media that contained a sugar composition corresponding to the wheat straw hydrolysate (Table 3).

Table 3. Volumetric productivity of of co-cultures of *C. owensensis* CO80 and *C. saccharolyticus* G5.

	Wheat straw hydrolysate with EB-1	**Defined medium with EB-1**	**Defined medium Modified DSM 640**
$Q_{glucose}$	1.88 ± 0.02	0.18 ± 0.16	0.09 ± 0.13
Q_{xylose}	2.64 ± 0.39	1.26 ±0.07	1.49 ± 0.25
$Q_{arabinose}$	0.18 ± 0.00	0.20 ± 0.00	0.16 ± 0.00
$Q_{acetate}$	4.74 ± 0.00	2.37 ± 0.37	2.63 ± 0.38
Q_{H2}	6.71 ± 0.06	2.47 ± 0.55	3.71 ± 0.42

Data adapted from Byrne et al. (2018)

Table 4. Population distribution of *C. owensensis* strain C80 and *C. saccharolyticus* G5 in continuous cultures.

Proportion	Strain G5	Strain C80
Wheat straw hydrolysate	99.76 ± 0.43%	0.24 ± 0.43%
Defined medium EB-1	99.91 ± 0.01 %	0.09 ± 0.01%
Defined medium DSM 640	98.45 ± 3.06 %	1.58 ± 3.17%

The population dynamics of co-cultures were analyzed to determine the stability of the co-cultures. As illustrated in Table 4, only a minute proportion of the co-culture consisted of *C. owensensis* CO80 in each case, thus *C. saccharolyticus* G5 dominated. However, a brief interruption of pH control during the co-culture on modified DSM 640 resulted in the population of CO80 exceeding 85% of the total population before returning to less than 1% after 2 volume changes. Although, low population numbers of planktonic CO80 were observed, a large quantity of biofilm occurred in all continuous cultivations particularly at the gas-liquid interface.

Discussion

In this study we successfully implemented ALE as strain development technique to improve the survival of *C. owensensis* in osmolarity-induced stress conditions.

Next to *C. saccharolyticus* (Pawar, 2014), this is the second *Caldicellulosiruptor* species to withstand higher osmolarities via adaptation. *C. owensensis* was successfully adapted to survive in 80 g/L glucose. However, not all *Caldicellulosiruptor* strains were as easily adaptable in our study. There were significant restrictions in the adaptation of *C. bescii, C. acetigenus* and *C. kristjanssonii* to higher sugar concentrations. *C. kristjanssonii* displayed a particular resistance to adaptation to higher osmolarities in glucose concentrations with a loss of viability above 30 g/l. Previously, a transcriptional analysis demonstrated that adaptation in *C. saccharolyticus* was a result of increased transposon activity as well as upregulation of proteins related to sugar transport (Pawar 2014). A recent study, (Sander et al., 2020), succeeded in developing two *C. bescii* strains possessing higher osmotolerance through genetic engineering. Analyses of these strains phenotypes resulted in that enhanced tolerance was accomplished through deletion of the FapR, a negative regulator of the fatty acid synthesis. Their analysis further hinted that mutations in regions of the genome of as yet unknown function, also increased osmotolerance, which demands validation. In short, evolvement of higher tolerance to osmotic potential may depend on expression of various (combinations of) genes and may even be species or strain dependent.

Although ALE increased osmotolerance, *C. owensensis* CO80 exhibits incomplete glucose consumption at elevated concentrations. This phenomenon has been previously observed in wild-type *C. saccharolyticus* (Pawar 2014). In addition, when cultivated on 80 g/L glucose, a significantly reduced volumetric hydrogen productivity was obtained compared to 10 and 30 g/L. Additionally, glucose uptake capacity was negatively affected, indicating that although *C. owensensis* is capable of surviving at 80 g/L, a significant loss of performance is observed.

The model was shown to be a useful tool to quantify the experimental observations. For instance, a high value of the OSM_{crit} parameter in the model indicated a higher tolerance to osmolarity, but the maximum capacity appeared to adjust with the osmolarity of the medium. In other words, the osmotolerance phenotype shifted in unison with the osmotic pressure of the environment, implicating the involvement of an active physiological mechanism. However, the presence of substrate inhibition, mainly in cultures at 30 g/L and 80 g/L glucose, may complicate further kinetic analysis of this phenomenon. Due to this inhibition, the apparent K_S value of the culture with 80 g/L glucose appeared to be four orders of magnitude higher than that of the cells in the culture of 10 g/L glucose (Equation 7) and in previous studies (Ciranna et al., 2014; Ljunggren et al., 2011; van Niel et al., 2003). This equation is adequate at low sugar concentrations, but it might not be sufficient to describe a fermentation with higher sugar concentrations. The calibrated K_S for the 80 g/L case is an "apparent K_S" which most probably constitutes of the "real K_S" multiplied by an inhibition factor. To counteract such a high K_S value, a second model, where K_S was a function of glucose, was used instead (Equation 1). This model gave a similar fit to the data for the 30 g/L and 80 g/L cultures. Furthermore, the inhibition due to osmolarity was of a higher significance than inhibition by the aqueous hydrogen concentration as analyzed in Figure 6.

When calibrating the parameters in the model to get a good fit to the experimental data, an initial start value of the parameter needs to be guesstimated. These values are of great importance for the end result as a poorly chosen initial value could result in a local minimum in the parameter estimation procedure, leading to a bad fit of the model to the experimental data and a faulty estimated parameter. To counteract this, the start values were initially chosen in proximity to the benchmark value from Ljunggren et al. (2011). When these values did not give the right fit to the experimental data, several new initial start values were tested as input in the *lsqcurvefit* function in MATLAB.

The reduction in Q_{H2} observed in batch fermentations is consistent with the data derived from Byrne et al. (2018) establishing that utilizing osmotolerant strains facilitated use of more concentrated hydrolysates albeit at the expense of Q_{H2}. In that study the Q_{H2} of the co-culture (6.71 ± 0.06 mmol/L/h) was lower than that observed in pure culture of the wild-type *C. saccharolyticus* grown on approximately threefold lower concentrated WSH containing 11 g/L monosaccharides (8.69 mmol/L/h) (Pawar et al., 2013). However, the Q_{H2} obtained with the defined DSM 640 medium was similar to that of wild-type *C. saccharolyticus* (4.2mmol/L/h) (de Vrije et al., 2007). Furthermore, the co-culture grown on WSH displayed a higher Q_{H2} when cultivated on wheat straw hydrolysate than on a defined medium. This confirms previous observations that *Caldicellulosiruptor* possesses a higher Q_{H2} when cultivated on wheat straw hydrolysate than on pure sugar (Pawar et al., 2013). This may be due to the presence of additional nutrients and/or oligosaccharides found in the wheat straw compared to that of the defined medium. The reduction of Q_{H2} compared to the wild-type *C. saccharolyticus* could be due to the presence of higher concentrations of inhibitory compounds that may reduce hydrogen productivity. *C. saccharolyticus* is sensitive to HMF and furfural concentrations above 1 and 2 g/L, respectively (de Vrije et al., 2009; Panagiotopoulos et al., 2010). Even though higher hydrolysate concentrations were used in the present study, only trace amounts of HMF and furfural were detected. The presence of, yet unknown, compounds in the hydrolysate could have resulted in the inhibition of *Caldicellulosiruptor*. Furthermore, higher concentrations of sugar intensified the occurrence of Maillard reactions, to which *Caldicellulosiruptor* species are very sensitive. A concentration of 80 g/l glucose led to significant browning of the cultivation media and resulted in failure of growth when the coloring arose before inoculation and was presumably also responsible for inconsistencies during cultivation at 30 g/L. Maillard products are known to inhibit the growth of other thermophilic bacterial species such as *Thermotoga* and

Thermoanaerobacter (de Vrije et al., 2009; Tomás et al., 2013). The presence of Maillard-based products will reduce the efficiency of any large-scale fermentation. One obvious choice for mitigating such reactions would be the omission of cysteine from the cultivation medium or by maintaining a low background sugar concentration in the culture through utilizing fed-batch or continuous cultures as modes of operation.

Additionally, the co-cultivation of *C. owensensis* CO80 and *C. saccharolyticus G5* resulted in a predominantly *C. saccharolyticus G5* population, with detection of only small quantities of *C. owensensis* CO80. Although, this could indicate cell mass washout of planktonic *C. owensensis* CO80. However, a large quantity of biofilm was observed in the bioreactors after termination of each cultivation. Due to that *C. owensensis* is known for its ability to form biofilm (Peintner et al., 2010) might point that *C. owensensis* CO80 remained significantly present in the fermentations in immobilized form.

Conclusions

The adaptation of *Caldicellulosiruptor* to higher osmotic conditions through ALE permitted survival at higher sugar concentrations, however, at the cost of Q_{H2}. Implementation of co-cultures of *C. owensensis* CO80 and *C. saccharolyticus* G5 facilitated cultivation of this genus in higher hydrolysate concentrations than previously reported, but even here reduced Q_{H2} were observed compared to wild-type *C. saccharolyticus* on dilute hydrolysate. It stands to reason that ALE leads to adaptation to the stress parameter to which its exposed, albeit at the expense of other desired traits. Therefore, a combination of ALE and metabolic engineering as applied in a Design, Build, Test and Learn cycle (Sandberg et al 2019) is a better strategy to construct the desired phenotype of a hydrogen cell factory. The kinetic models developed herein, were able to predict the behavior of growth of

CO80 when exposed to 10 and 30 g/L of glucose. The slight overestimation in the models and the growth kinetics of cultures at 80 g/L glucose illustrates that this is the critical boundary beyond which this strain possesses no further capacity for adaptation.

In contrast to *C. saccharolyticus* (Pawar et al., 2013), *C. owensensis* cannot be cultivated without cysteine, as this species lacks the sulfur assimilation pathway (Pawar & van Niel, 2014). Therefore, co-cultivations of these two species in the absence of cysteine, but with sulfate as the sole sulfur source, could be of interest. In addition, co-cultivation of wild-type strains of *C. saccharolyticus* and *C. owensensis* could also stimulate biofilm formation (Pawar et al., 2015). However, this study demonstrated that *C. saccharolyticus* G5 strain completely overtook the *C. owensensis* CO80 strain in the co-cultivations. Although this observation can be considered discouraging, large quantities of biofilm occurred indicating the presence of *C. owensensis* CO80. Therefore, alternative reactor systems should be applied to enhance biofilm formation, thereby improving cell mass retention that will contribute to higher Q_{H2}. The co-culture can possible be a strategy to increase the robustness of the bioreactor performance since we observed that CO80 took over at conditions when the bioreactor was acidified. However, for industrial application the properties of CO80 to reach higher hydrogen productivities need to be significantly improved.

Material and Methods

Strains and cultivation medium

The wild-type strains of *Caldicellulosiruptor owensensis* DSM 13100, *Caldicellulosiruptor kronotskyensis* DSM 18902, *Caldicellulosiruptor* bescii DSM 6725*, Caldicellulosiruptor acetigenus* DSM 7040 and *Caldicellulosiruptor kristjanssonii* DSM 12137 were obtained from the Deutsche Sammlung von

Mikroorganismen und Zellkulturen (DSMZ; Braunschweig, Germany). Subcultivations were conducted in 250 mL serum flasks with 50 mL modified DSM 640 media (Willquist et al., 2009) with the addition of 50 mM HEPES and 10 g/L glucose, unless otherwise stated. A 1000x vitamin solution was prepared as per Zeidan and van Niel (2010) and a modified SL-10 solution was prepared described previously (Pawar & van Niel, 2014).

Adaptation of species to higher osmolarity

Adaptation of *C. owensensis, C. kronotsyensis, C. bescii, C. acetigenus and C. kristjanssonii* to higher osmolarity was performed through adaptive laboratory evolution that initially involved repeated sub-cultivation of each strain in a modified DSM 640 medium containing 10 g/L of glucose. The glucose concentration was increased in 10 g/L increments when generation time for each strain was less than 0.4 h^{-1} and OD was above 0.3. This sequential increase of glucose concentration was continued until no growth in higher glucose concentrations was observed (Pawar, 2014).

Fermentor set-up

Batch cultivations were performed in a jacketed, 3-L fermentor equipped with an ADI 1025 Bio-Console and ADI 1010 Bio-Controller (Applikon, Schiedam, The Netherlands). A working volume of 1L was used in all batch cultivations and the pH was maintained at 6.5 ± 0.1 by automatic titration with 4 M NaOH. The temperature was thermostatically kept at 70 ± 1^{o}C. Stirring was maintained at 250 rpm and nitrogen was sparged through the medium at a rate of 6 L/h. A water-cooled condenser was utilised (4^{o}C) to prevent the evaporation of the medium. During each cultivation, samples were collected at regular intervals for HPLC and to monitor optical density. The supernatant from each sample was collected and stored at -20^{o}C for further quantification of sugars, organic acids, and ethanol. Gas samples were collected from the headspace of the fermentor to

quantify H_2 and CO_2. Analysis of osmotolerant *C. owensensis* CO80 was performed using both batch cultivations with the addition of 10, 30 and 80 g/L of glucose. Each of the batch cultivation was conducted in duplicate except for 30 g/L which was performed in triplicate. Co-culturing of *C. owensensis* C80 and *C. saccharolyticus* G5 in continuous cultures were performed in a previous study (Byrne et al 2018) at a dilution rate of 0.05 h^{-1}. Three different media were used: defined media (modified DSM 640 and EB-1) and wheat straw hydrolysate (for media compositions see Byrne et al (2018)). Biomass samples were taken for population dynamics during steady state situations.

Analytical methods

Optical density was determined using an Ultraspec 2100 pro spectrophotometer (Amersham Biosciences) at 620 nm.

Sugars and organic acids were detected using HPLC (Waters, Milford, MA, USA). For the quantification of organic acids, and ethanol, a HPLC was used equipped with an Aminex HPX-87H ion exchange column (Bio-Rad, Hercules, USA) at 60 °C with 5 mM H_2SO_4 as mobile phase at a flow rate of 0.6 mL/min. Glucose, xylose and arabinose quantification was conducted using a HPLC with two Shodex SP-0810 Columns (Shodex, Japan) in series with water as a mobile phase at a flow rate of 0.6 ml/min.

H_2 and CO_2 concentrations were quantified with an Agilent 7890B Series GC (Agilent GC 7890, Santa Clara, CA) equipped with a TCD detector and a ShinCarbon ST 50/80 UM (2m x 1/16" x 1mm) column. Helium carrier gas was employed, at a flow rate of 10 ml/min. During operation, an initial oven temperature of 80°C was maintained for 1 min followed by a temperature ramp of 20°C/min for 4 min with a subsequent 2 min hold time at 160°C.

Determination of population dynamics

DNA was extracted from 2mL of frozen cell pellets -using the GeneJet Genomic DNA purification kit (Thermofisher, Waltham, MA, USA). qPCR was carried out by amplification of genomic DNA with primers (Table 5) targeting single copy non-homologous regions of *C. saccharolyticus* and *C. owensensis.*

Table 5: PCR primers for *C. saccharolyticus* and *C. owensensis* differentiation**.**

Species	Primer	Seqeunce
C. owensensis	Cowen_F1	5' - GGCAAGTGGGAAGAAGATGA – 3'
C. owensensis	Cowen_R1	5' - CTCCGCAAGACTTGAACACA – 3'
C. saccharolyticus	Csacc_F1	5' - TATTATGGGGATTGGGACGA – 3'
C. saccharolyticus	Csacc_R1	5' - CTGGCGCACCAAAGATAAAT – 3'

Sequences were obtained through multiple genome alignment using Mauve (Darling et al., 2004). qPCR reactions were conducted using DreamTaq DNA polymerase (Thermofisher, Waltham, MA, USA) and EvaGreen® Dye (Biotium, Fremont, CA) in a BioRad CFX96 Realtime PCR (BioRad, Herculus, CA, USA) machine. The Quantification cycle (Cq) values and melting curve analysis were determined using the CFX Manager™ software 3.1 (Bio-Rad, Hercules, CA, USA). The copy numbers obtained in the software by absolute quantification were in relation to defined standard concentrations (0.02 to 20 ng/µl) obtained from known quantities of genomic DNA obtained from pure cultures. The sum of

558 calculated copy number values was used to determine the relative population of
559 the different species. The following PCR conditions were used: Denaturation
560 95°C 7 min; 32 cycles of 95°C 30 s, 54°C and 56°C for *C. owensensis* and *C*
561 *saccharolyticus*, respectively, for 30 s, 70°C 20 s; melting curve analysis: 65°C
562 30 s hold time, ramp to 95°C with 0.05°C/s. Each sample was analysed in
563 biological duplicates.

564

565 **Mathematical modelling**

566 To quantify and evaluate the effect of the osmotolerant strains, a kinetic
567 mathematical model was adapted from Ljunggren et al. (2011) and run in
568 MATLAB R2017a (Mathworks, USA). The model was set up on a molar basis
569 containing mathematical expressions for microbial growth, substrate
570 consumption, product formation and gas to liquid mass transfer. The model was
571 used with a few alterations to the mass balance equations. The mass balances of
572 the gaseous compounds hydrogen and carbon dioxide are expressed as a change
573 in concentration (mol/L) over time instead of a change in flow over time. This is
574 similar to what has been described in (Björkmalm et al., 2018) and given as the
575 following equations:

576

577 $$\frac{dH_{2,g}}{dt} = \frac{V_{liq}}{V_{gas}} * \rho_{t,H_2} + (-H_{2,g} \cdot \frac{q_{gas}}{V_{gas}}) \quad (2)$$

578

579 $$\frac{dCO_{2,g}}{dt} = \frac{V_{liq}}{V_{gas}} * \rho_{t,CO_2} + (-CO_{2,g} \cdot \frac{q_{gas}}{V_{gas}}) \quad (3)$$

580

581

582 where V_{liq} and V_{gas} are the liquid and the gas volumes (L), respectively, q_{gas} is the
583 total gas flow (L/h), $H_{2,g}$ is gaseous hydrogen (mol/L), CO_2 is gaseous carbon

584 dioxide (mol/L), $\rho_{t,H2}$ and $\rho_{t,CO2}$ are the mass transfer rate of hydrogen and carbon
585 dioxide respectively (mol/L/h).

586 The osmolarity expression, Eq 5, is calculated in the same way as Ljunggren et
587 al. (2011), except that $CO_{2,sol}$, i.e., the CO_2 ionic species (bicarbonate and
588 carbonate), is excluded since these were not measured experimentally. This is
589 further motivated by the fact that, according to model calculations in the current
590 study, $CO_{2,sol}$ constituted to less than 2% of the total osmolarity.

591

592 $$OSM = Glu + 2 \cdot Ac + 2 \cdot Lac + 0.08 \quad (4)$$

593

594 where Glu, Ac and Lac are the concentrations of glucose, acetate and lactate,
595 respectively. 0.08 is the estimated background osmolarity of the medium and it is
596 adjusted slightly in comparison to the benchmark value from Ljunggren et al.
597 (2011). The background osmolarity has not been experimentally measured in this
598 case. The stochiometric factor 2 implies that for each mole of acid produced, one
599 mole of NaOH is included that was added to maintain the pH.

600 The inhibition due to osmolarity and dissolved hydrogen concentration is
601 expressed as (Ljunggren et al., 2011):

602

603 $$I_{osm} = 1 - (\frac{OSM}{OSM_{crit}})^{n_\mu} \quad (5)$$

604

605 $$I_{H_{2,aq}} = 1 - \left(\frac{H_{2,aq}}{H_{2,aq,crit}}\right)^{n_{H_2}} \quad (6)$$

606

607 which are implemented in the growth kinetic equation:

608 $$\mu = \mu_{max} \cdot \frac{S}{S+K_s} \cdot I_{osm} \cdot I_{H_{2,aq}} \quad (7)$$

609

where n_{μ} and n_{H2} are exponential parameters describing the degree of inhibition and OSM_{crit} (mol/L) and $H_{2,aq,crit}$ (mol/L) are the critical osmolarity and critical dissolved hydrogen concentration, respectively. OSM_{crit} is central in this context where a high value of OSM_{crit} indicates a high tolerance for osmolarity. μ (h^{-1}) is the specific growth rate, μ_{max} (h^{-1}) is the maximum specific growth rate, K_S (mol/L) is the affinity constant for glucose and S (mol/L) is the concentration of glucose. The mass balance equation for the biomass X consists of the rate of glucose consumption r_s (cmol/L/h), with $Y_{S,X}$ (cmol/mol) as the yield of biomass from glucose, and the cell death rate, r_{cd} (h^{-1}), which is based on first-order kinetics.

The model was evaluated against different batch experimental data. To fit the model to experimental data a parameter calibration was conducted using the function *lsqcurvefit* in MATLAB. This function solves the nonlinear curve-fitting problem using the least-square method. The parameters considered to be of greatest importance were μ_{max}, OSM_{crit}, r_{cd}, $Y_{S,H2}$ (H_2 yield coefficient, mol H_2/mol glucose), n_{μ} and n_{H2}. The MATLAB function *nlparci* was used to calculate the 95% confidence interval for the calibrated parameters to assess their uncertainties.

To assess the accuracy of the model in relation to the experimental data, R^2 values and curve slope values were calculated. This was done by plotting the simulated values against the experimental values followed by a linear regression which gave the R^2 value as well as the linear equation $y = k \cdot x$, where k is the curve slope value.

The biomass yield coefficient $Y_{S,X}$ was calculated using the experimental data but altered in the 80 g/L model to fit the experimental data. The yields for hydrogen, acetate, lactate and carbon dioxide used in the model, $Y_{S,H2}$, $Y_{S,Ac}$, $Y_{S,Lac}$ and $Y_{S,CO2}$, were based on stoichiometry according to:

$C_6H_{12}O_6 + 2H_2O \rightarrow 2C_2H_4O_2 + 2CO_2 + 4H_2$ (8)

$C_6H_{12}O_6 \rightarrow 2C_3H_6O_3$ (9)

Declarations

Not applicable

Ethics approval and consent to participate

Not applicable

Consent for publication

Not applicable.

Availability of data and materials

All data generated or analyzed during this study are included in this article. If additional information is needed, please contact the corresponding author.

Competing interests

The authors declare that they have no competing interests.

Funding

This study was funded by the Swedish Energy Agency (Metanova project no 31090-2), Formas (HighQH2, 2017-00795) and Vinnova (Multibio, 2017-03286) – Sweden's Innovation Agency of which neither participated in the execution of the study or in the manuscript writing.

Authors' contributions

EB: design, operation and supervision fermentation processes, metabolite analysis and manuscript writing.

JB: data analysis, calculations, model development and manuscript writing.

JPB: fermentation processes, metabolite analysis and manuscript review

KS: development of genetic protocol and manuscript review.

KW: supervision of modelling, analysis and fermentation and manuscript writing.

EvN: supervision of fermentation processes, modelling, analysis and manuscript writing.

Corresponding author
Correspondence to ed.van_niel@tmb.lth.se

Author details
Current address EB: Ballintober, Hollywood, Co. Wicklow, W91 RDP3, Ireland and JPB: Coriolis Pharma Research GmbH, Fraunhoferstrasse 18B, 82152 Planegg, Germany.

Acknowledgements
The authors are grateful to the 3 Swedish funding agencies, Swedish Energy Agency, Formas and Vinnova for funding this research.

References

Azimian, L., Bassi, A., Mercer, S.M. 2019. Investigation of growth kinetics of Debaryomyces hansenii (LAF-3 10 U) in petroleum refinery desalter effluent. *The Canadian Journal of Chemical Engineering*, **97**(1), 27-31.

Azwar, M.Y., Hussain, M.A., Abdul-Wahab, A.K. 2014. Development of biohydrogen production by photobiological, fermentation and electrochemical processes: A review. *Renewable and Sustainable Energy Reviews*, **31**, 158-173.

Björkmalm, J., Byrne, E., van Niel, E.W.J., Willquist, K. 2018. A non-linear model of hydrogen production by *Caldicellulosiruptor saccharolyticus* for diauxic-like consumption of lignocellulosic sugar mixtures. *Biotechnology for Biofuels*, **11**(1), 175.

Byrne, E., Kovacs, K., van Niel, E.W.J., Willquist, K., Svensson, S.-E., Kreuger, E. 2018. Reduced use of phosphorus and water in sequential dark fermentation and anaerobic digestion of wheat straw and the application of ensiled steam-pretreated lucerne as a macronutrient provider in anaerobic digestion. *Biotechnology for Biofuels*, **11**(1), 281.

Ciranna, A., Ferrari, R., Santala, V., Karp, M. 2014. Inhibitory effects of substrate and soluble end products on biohydrogen production of the alkalithermophile Caloramator celer: Kinetic, metabolic and transcription analyses. *International Journal of Hydrogen Energy*, **39**(12), 6391-6401.

Claassen, P.A.M., van Lier, J.B., Lopez Contreras, A.M., van Niel, E.W.J., Sijtsma, L., Stams, A.J.M., de Vries, S.S., Weusthuis, R.A. 1999. Utilisation of biomass for the supply of energy carriers. *Applied Microbiology and Biotechnology*, **52**(6), 741-755.

Darling, A.C.E., Mau, B., Blattner, F.R., Perna, N.T. 2004. Mauve: multiple alignment of conserved genomic sequence with rearrangements. *Genome research*, **14**(7), 1394-1403.

de Vrije, T., Bakker, R.R., Budde, M.A., Lai, M.H., Mars, A.E., Claassen, P.A. 2009. Efficient hydrogen production from the lignocellulosic energy crop Miscanthus by the extreme thermophilic bacteria *Caldicellulosiruptor saccharolyticus* and *Thermotoga neapolitana*. *Biotechnology for Biofuels*, **2**(1), 12.

de Vrije, T., Mars, A.E., Budde, M.A.W., Lai, M.H., Dijkema, C., de Waard, P., Claassen, P.A.M. 2007. Glycolytic pathway and hydrogen yield studies of the extreme thermophile *Caldicellulosiruptor saccharolyticus*. *Applied Microbiology and Biotechnology*, **74**(6), 1358.

Dötsch, A., Severin, J., Alt, W., Galinski, E.A., Kreft, J.-U. 2008. A mathematical model for growth and osmoregulation in halophilic bacteria. *Microbiology*, **154**(10), 2956-2969.

Dragosits, M., Mattanovich, D. 2013. Adaptive laboratory evolution – principles and applications for biotechnology. *Microbial Cell Factories*, **12**(1), 64.

European Parliament and Council. 2015. Directive (EU) 2015/1513 of the European parliament and of the council of 9 September 2015 amending Directive 98/70/EC relating to the quality of petrol and diesel fuels and amending Directive 2009/28/EC on the promotion of the use of energy from renewable sources, Official Journal of the European Union.

Foglia, D., Ljunggren, M., Wukovits, W., Friedl, A., Zacchi, G., Urbaniec, K., Markowski, M. 2010. Integration studies on a two-stage fermentation process for the production of biohydrogen. *Journal of Cleaner Production*, **18**, S72-S80.

Gonçalves, L.G., Borges, N., Serra, F., Fernandes, P.L., Dopazo, H., Santos, H. 2012. Evolution of the biosynthesis of di-myo-inositol phosphate, a marker of adaptation to hot marine environments. *Environmental Microbiology*, **14**(3), 691-701.

Kempf, B., Bremer, E. 1998. Uptake and synthesis of compatible solutes as microbial stress responses to high-osmolality environments. *Arch Microbiol*, **170**(5), 319-30.

Ljunggren, M., Willquist, K., Zacchi, G., van Niel, E.W. 2011. A kinetic model for quantitative evaluation of the effect of hydrogen and osmolarity on hydrogen production by *Caldicellulosiruptor saccharolyticus*. *Biotechnology for Biofuels*, **4**(1), 31.

Ljunggren, M., Zacchi, G. 2010. Techno-economic analysis of a two-step biological process producing hydrogen and methane. *Bioresource Technology*, **101**(20), 7780-7788.

Martins, L.O., Santos, H. 1995. Accumulation of Mannosylglycerate and Di-myo-Inositol-Phosphate by Pyrococcus furiosus in Response to Salinity and Temperature. *Applied and Environmental Microbiology*, **61**(9), 3299-3303.

Nunes, O.C., Manaia, C.M., Da Costa, M.S., Santos, H. 1995. Compatible Solutes in the Thermophilic Bacteria Rhodothermus marinus and "Thermus thermophilus". *Applied and Environmental Microbiology*, **61**(6), 2351-2357.

Panagiotopoulos, I.A., Bakker, R.R., de Vrije, T., Koukios, E.G., Claassen, P.A.M. 2010. Pretreatment of sweet sorghum bagasse for hydrogen production by

Caldicellulosiruptor saccharolyticus. *International Journal of Hydrogen Energy*, **35**(15), 7738-7747.

Pawar, S.S. 2014. *Caldicellulosiruptor saccharolyticus*: an Ideal Hydrogen Producer? in: *Faculty of Engineering, LTH*, Vol. PhD Thesis, Lund University. Lund.

Pawar, S.S., Nkemka, V.N., Zeidan, A.A., Murto, M., van Niel, E.W.J. 2013. Biohydrogen production from wheat straw hydrolysate using *Caldicellulosiruptor saccharolyticus* followed by biogas production in a two-step uncoupled process. *International Journal of Hydrogen Energy*, **38**(22), 9121-9130.

Pawar, S.S., van Niel, E.W.J. 2014. Evaluation of assimilatory sulphur metabolism in *Caldicellulosiruptor saccharolyticus*. *Bioresource Technology*, **169**, 677-685.

Pawar, S.S., Vongkumpeang, T., Grey, C., van Niel, E.W. 2015. Biofilm formation by designed co-cultures of *Caldicellulosiruptor* species as a means to improve hydrogen productivity. *Biotechnology for Biofuels*, **8**(1), 19.

Peabody, G., Winkler, J., Fountain, W., Castro, D.A., Leiva-Aravena, E., Kao, K.C. 2016. Benefits of a Recombination-Proficient *Escherichia coli* System for Adaptive Laboratory Evolution. *Applied and environmental microbiology*, **82**(22), 6736-6747.

Peintner, C., Zeidan, A.A., Schnitzhofer, W. 2010. Bioreactor systems for thermophilic fermentative hydrogen production: evaluation and comparison of appropriate systems. *Journal of Cleaner Production*, **18**, S15-S22.

Rainey, F.A., Donnison, A.M., Janssen, P.H., Saul, D., Rodrigo, A., Bergquist, P.L., Daniel, R.M., Stackebrandt, E., Morgan, H.W. 1994. Description of *Caldicellulosiruptor saccharolyticus* gen. nov., sp. nov: An obligately anaerobic, extremely thermophilic, cellulolytic bacterium. *FEMS Microbiology Letters*, **120**(3), 263-266.

Rodrigues, M.V., Borges, N., Almeida, C.P., Lamosa, P., Santos, H. 2009. A Unique β-1,2-Mannosyltransferase of *Thermotoga maritima* That Uses Di-*myo*-Inositol Phosphate as the Mannosyl Acceptor. *Journal of Bacteriology*, **191**(19), 6105-6115.

Sander, K.B., Chung, D., Klingeman, D.M., Giannone, R.J., Rodriguez, M., Whitham, J., Hettich, R.L., Davison, B.H., Westpheling, J., Brown, S.D. 2020. Gene targets for engineering osmotolerance in Caldicellulosiruptor bescii. *Biotechnology for Biofuels*, **13**(1), 50.

Sanderson, K. 2011. Lignocellulose: A chewy problem. *Nature*, **474**, S12.

Schleifer, K.-H. 2009. Phylum XIII. Firmicutes Gibbons and Murray 1978, 5 (Firmacutes [sic] Gibbons and Murray 1978, 5). in: *Bergey's Manual® of Systematic Bacteriology*, Springer, pp. 19-1317.

Sims, R., Taylor, M., Saddler, J., Mabee, W. 2008. From 1st-to 2nd-generation biofuel technologies. *Paris: International Energy Agency (IEA) and Organisation for Economic Co-Operation and Development*.

Sivakumar, A., Srinivasaraghavan, T., Swaminathan, T., Baradarajan, A. 1994. Extended monod kinetics for substrate inhibited systems. *Bioprocess Engineering*, **11**(5), 185-188.

Tomás, A.F., Karakashev, D., Angelidaki, I. 2013. Thermoanaerobacter pentosaceus sp. nov., an anaerobic, extremely thermophilic, high ethanol-yielding bacterium

isolated from household waste. *International Journal of Systematic and Evolutionary Microbiology*, **63**(7), 2396-2404.

van Niel, E.W.J., Claassen, P.A.M., Stams, A.J.M. 2003. Substrate and product inhibition of hydrogen production by the extreme thermophile, *Caldicellulosiruptor saccharolyticus*. *Biotechnol Bioeng*, **81**.

VanFossen, A.L., Verhaart, M.R.A., Kengen, S.M.W., Kelly, R.M. 2009. Carbohydrate Utilization Patterns for the Extremely Thermophilic Bacterium *Caldicellulosiruptor saccharolyticus* Reveal Broad Growth Substrate Preferences. *Applied and Environmental Microbiology*, **75**(24), 7718-7724.

Willquist, K., Claassen, P.A.M., van Niel, E.W.J. 2009. Evaluation of the influence of CO_2 on hydrogen production by *Caldicellulosiruptor saccharolyticus*. *International Journal of Hydrogen Energy*, **34**(11), 4718-4726.

Zeidan, A.A., van Niel, E.W.J. 2010. A quantitative analysis of hydrogen production efficiency of the extreme thermophile *Caldicellulosiruptor owensensis* OLT. *International Journal of Hydrogen Energy*, **35**(3), 1128-1137.

Figure legends

Figure 1. Development of osmotolerant strains of *C. owensensis, C. kronotskyensis, C. bescii, C. acetigenus* and *C. kristjanssonii*. Values in green indicate osmotolerant adaptation steps were completed on stated concentrations of glucose. Values in yellow indicate the final osmotolerant development step and therefore the highest concentration of glucose that the strains can be grown.

Figure 2. Experimental data (discrete points) and modelling results (lines) for the 10 g/L glucose cultures. Upper left: glucose consumption, acetate and lactate production. Upper right: biomass production. Lower left: hydrogen productivity. Lower right: accumulated hydrogen production.

Figure 3. Experimental data (discrete points) and modelling results (lines) for the 30 g/L glucose cultures. Upper left: glucose consumption, acetate and lactate production. Upper right: biomass production. Lower left: hydrogen productivity. Lower right: accumulated hydrogen production.

Figure 4. Experimental data (discrete points) and modelling results (lines) for the 80 g/L glucose cultures. Upper left: glucose consumption, acetate and lactate production. Upper right: biomass production. Lower left: hydrogen productivity. Lower right: accumulated hydrogen production.

Figure 5. Comparison of the calibrated parameters OSM_{crit} (orange) and K_s (grey).

Figure 6. Simulated values of I_{osm} and $I_{H2,aq}$ for the different models.

Figure 1

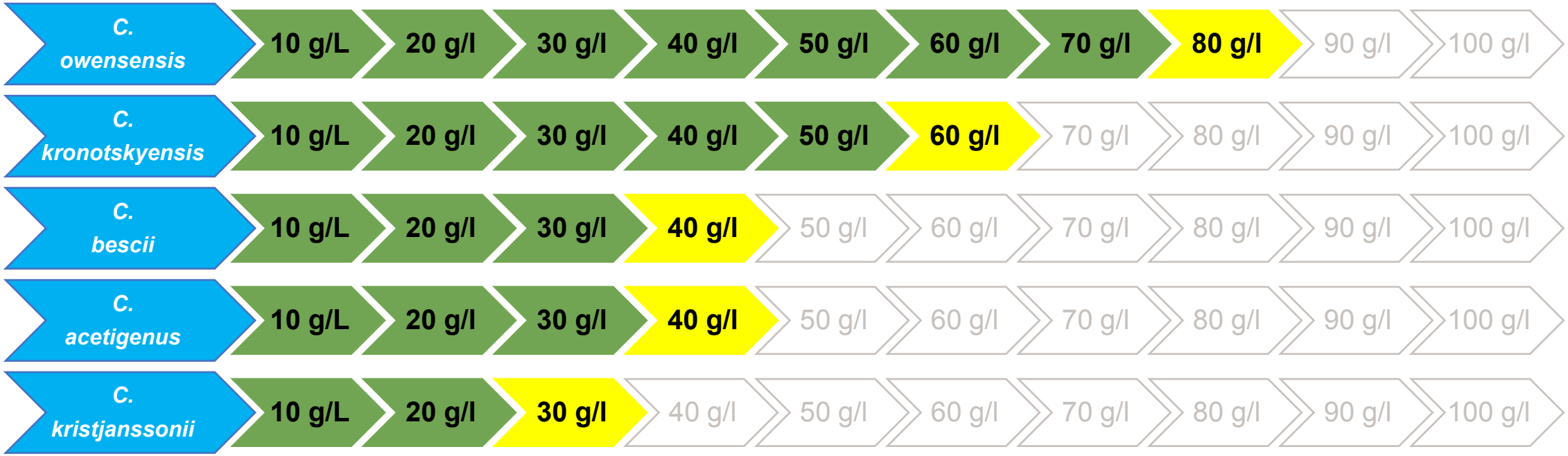
C. owensensis
10 g/L
20 g/l
30 g/l
40 g/l
50 g/l
60 g/l
70 g/l
80 g/l
90 g/l
100 g/l
C. kronotskyensis
10 g/L
20 g/l
30 g/l
40 g/l
50 g/l
60 g/l
70 g/l
80 g/l
90 g/l
100 g/l
C. bescii
10 g/L
20 g/l
30 g/l
40 g/l
50 g/l
60 g/l
70 g/l
80 g/l
90 g/l
100 g/l
C. acetigenus
10 g/L
20 g/l
30 g/l
40 g/l
50 g/l
60 g/l
70 g/l
80 g/l
90 g/l
100 g/l
C. kristjanssonii
10 g/L
20 g/l
30 g/l
40 g/l
50 g/l
60 g/l
70 g/l
80 g/l
90 g/l
100 g/l

Figure 2

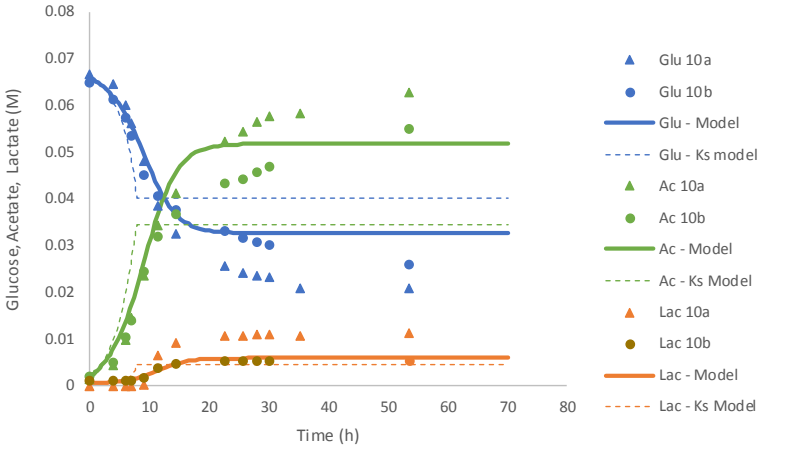
Glucose, Acetate, Lactate (M)
Time (h)
Glu 10a
Glu 10b
Glu - Model
Glu - Ks model
Ac 10a
Ac 10b
Ac - Model
Ac - Ks Model
Lac 10a
Lac 10b
Lac - Model
Lac - Ks Model

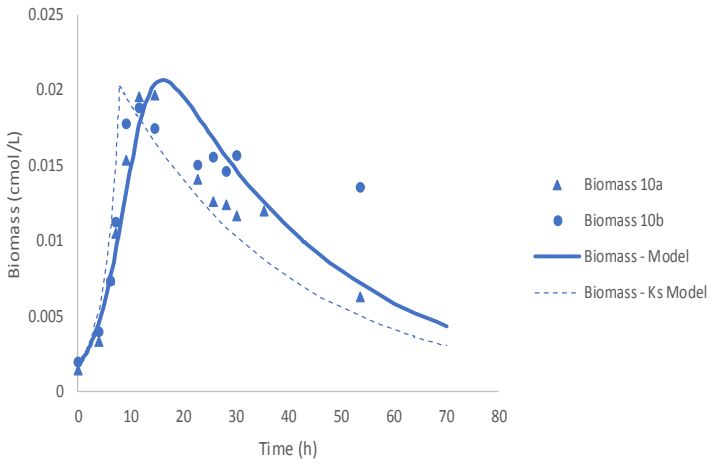
Biomass (cmol/L)
Time (h)
Biomass 10a
Biomass 10b
Biomass - Model
Biomass - Ks Model

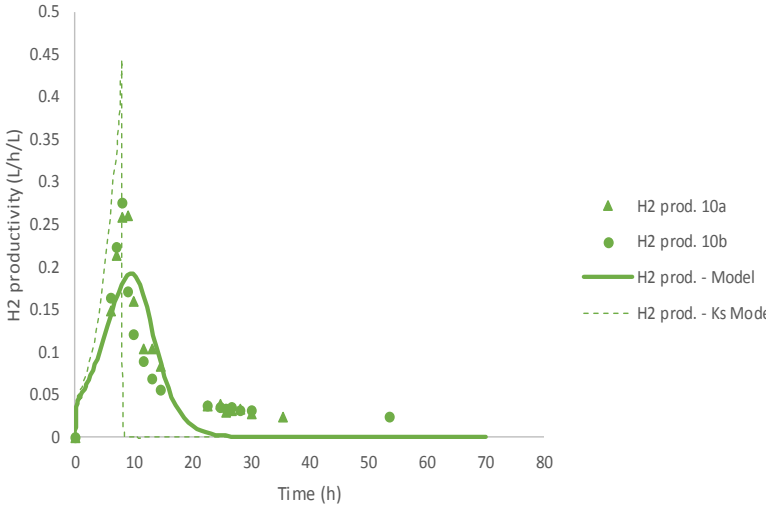
H2 productivity (L/h/L)
Time (h)
H2 prod. 10a
H2 prod. 10b
H2 prod. - Model
H2 prod. - Ks Mode

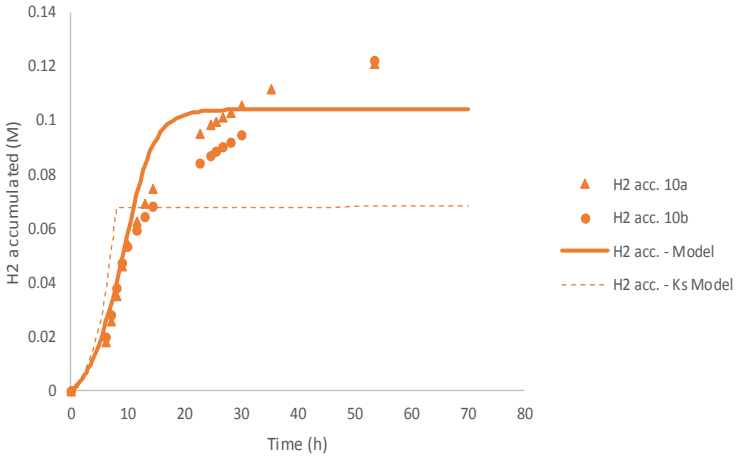
H2 accumulated (M)
Time (h)
H2 acc. 10a
H2 acc. 10b
H2 acc. - Model
H2 acc. - Ks Model

Figure 3

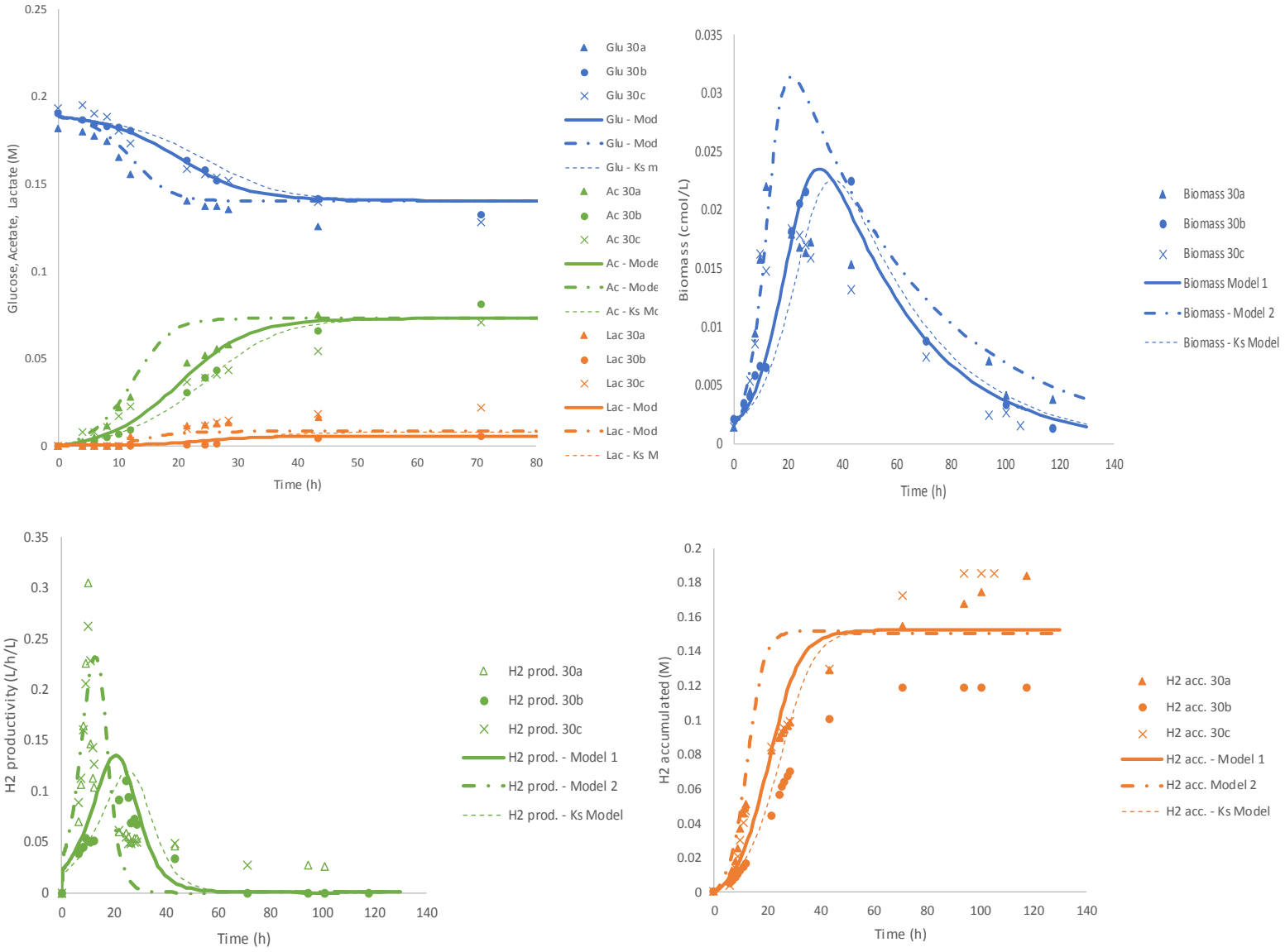
Glucose, Acetate, Lactate (M)
Time (h)
Glu 30a
Glu 30b
Glu 30c
Glu - Mod
Glu - Mod
Glu - Ks m
Ac 30a
Ac 30b
Ac 30c
Ac - Mode
Ac - Mode
Ac - Ks Mc
Lac 30a
Lac 30b
Lac 30c
Lac - Mod
Lac - Mod
Lac - Ks M
Biomass (cmol/L)
Time (h)
Biomass 30a
Biomass 30b
Biomass 30c
Biomass Model 1
Biomass - Model 2
Biomass - Ks Model
H2 productivity (L/h/L)
Time (h)
H2 prod. 30a
H2 prod. 30b
H2 prod. 30c
H2 prod. - Model 1
H2 prod. - Model 2
H2 prod. - Ks Model
H2 accumulated (M)
Time (h)
H2 acc. 30a
H2 acc. 30b
H2 acc. 30c
H2 acc. - Model 1
H2 acc. Model 2
H2 acc. - Ks Model

Figure 4

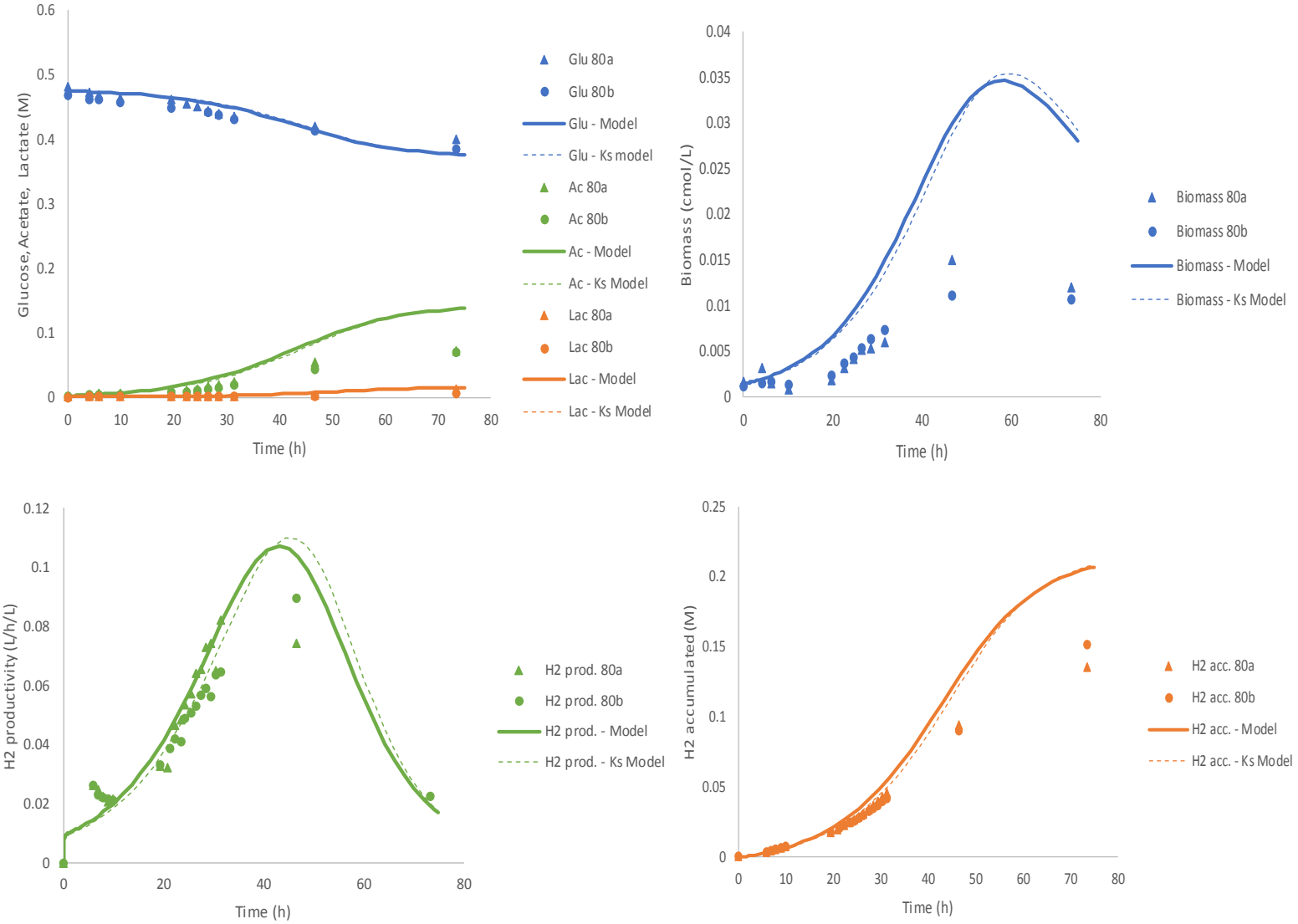
Glucose, Acetate, Lactate (M)
Time (h)
Glu 80a
Glu 80b
Glu - Model
Glu - Ks model
Ac 80a
Ac 80b
Ac - Model
Ac - Ks Model
Lac 80a
Lac 80b
Lac - Model
Lac - Ks Model
Biomass (cmol/L)
Time (h)
Biomass 80a
Biomass 80b
Biomass - Model
Biomass - Ks Model
H2 productivity (L/h/L)
Time (h)
H2 prod. 80a
H2 prod. 80b
H2 prod. - Model
H2 prod. - Ks Model
H2 accumulated (M)
Time (h)
H2 acc. 80a
H2 acc. 80b
H2 acc. - Model
H2 acc. - Ks Model

Figure 5

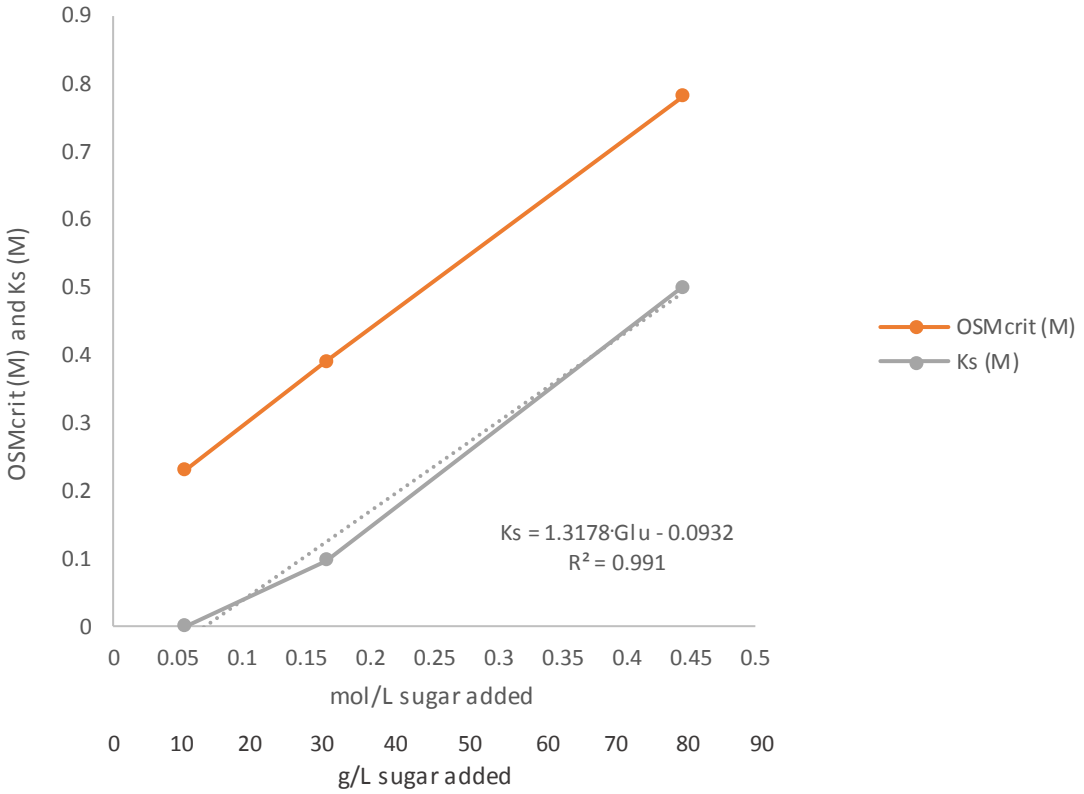
0.9
0.8
0.7
0.6
0.5
0.4
0.3
0.2
0.1
0
OSMcrit (M) and Ks (M)
Ks = 1.3178·Glu - 0.0932
R² = 0.991
0
0.05
0.1
0.15
0.2
0.25
0.3
0.35
0.4
0.45
0.5
mol/L sugar added
0
10
20
30
40
50
60
70
80
90
g/L sugar added
OSMcrit (M)
Ks (M)

Figure 6

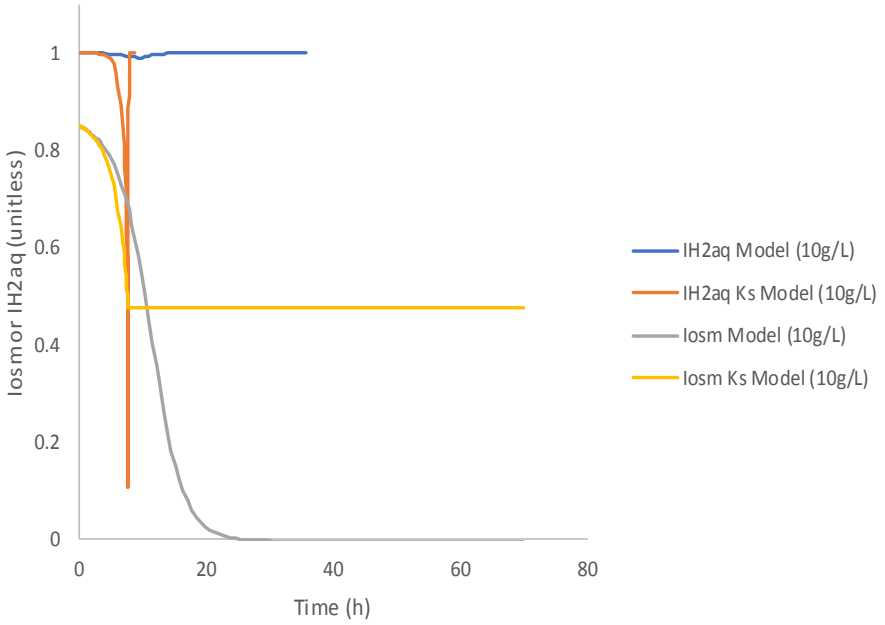
Iosmor IH2aq (unitless)
1
0.8
0.6
0.4
0.2
0
0
20
40
60
80
Time (h)
IH2aq Model (10g/L)
IH2aq Ks Model (10g/L)
Iosm Model (10g/L)
Iosm Ks Model (10g/L)

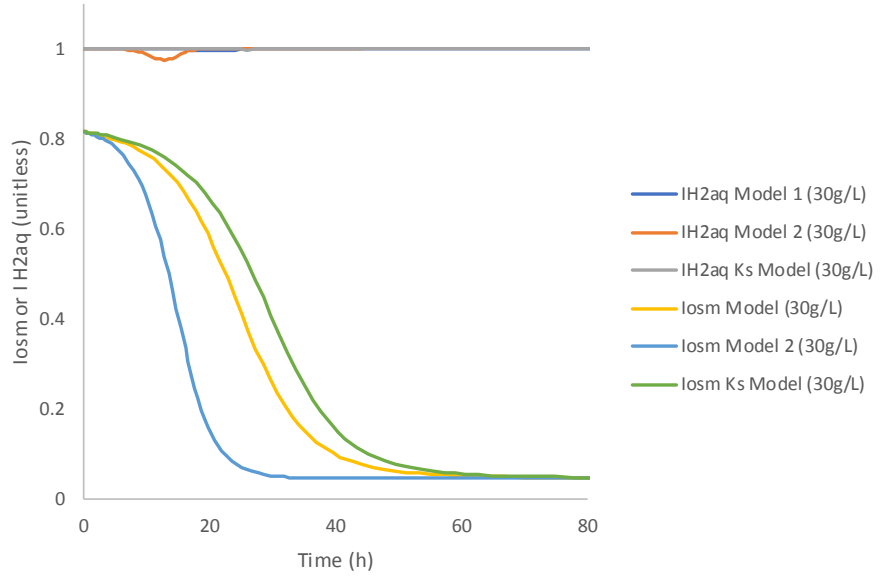
Iosmor I H2aq (unitless)
1
0.8
0.6
0.4
0.2
0
0
20
40
60
80
Time (h)
IH2aq Model 1 (30g/L)
IH2aq Model 2 (30g/L)
IH2aq Ks Model (30g/L)
Iosm Model (30g/L)
Iosm Model 2 (30g/L)
Iosm Ks Model (30g/L)

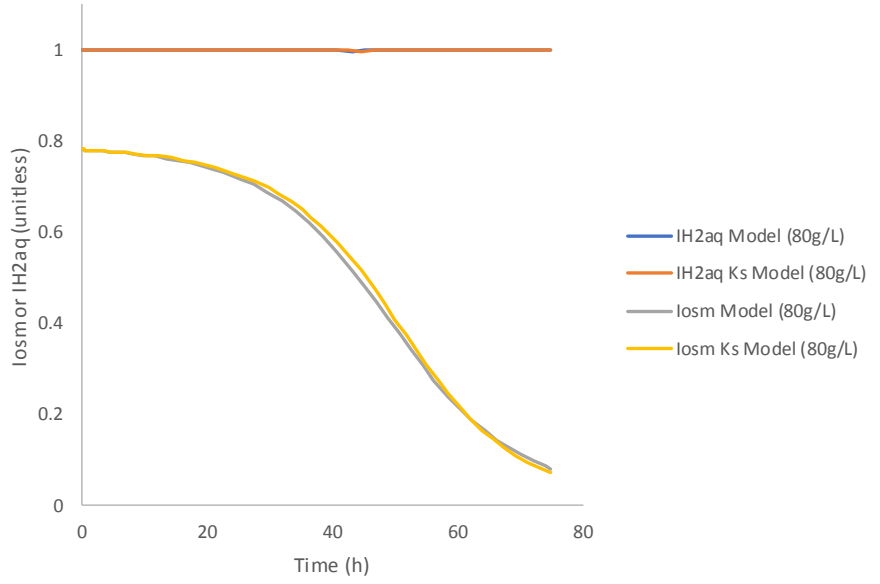
Iosmor IH2aq (unitless)
1
0.8
0.6
0.4
0.2
0
0
20
40
60
80
Time (h)
IH2aq Model (80g/L)
IH2aq Ks Model (80g/L)
Iosm Model (80g/L)
Iosm Ks Model (80g/L)

Figures

Figure 1

Development of osmotolerant strains of C. owensensis, C. kronotskyensis, C. bescii, C. acetigenus and C. kristjanssonii. Values in green indicate osmotolerant adaptation steps were completed on stated concentrations of glucose. Values in yellow indicate the final osmotolerant development step and therefore the highest concentration of glucose that the strains can be grown.

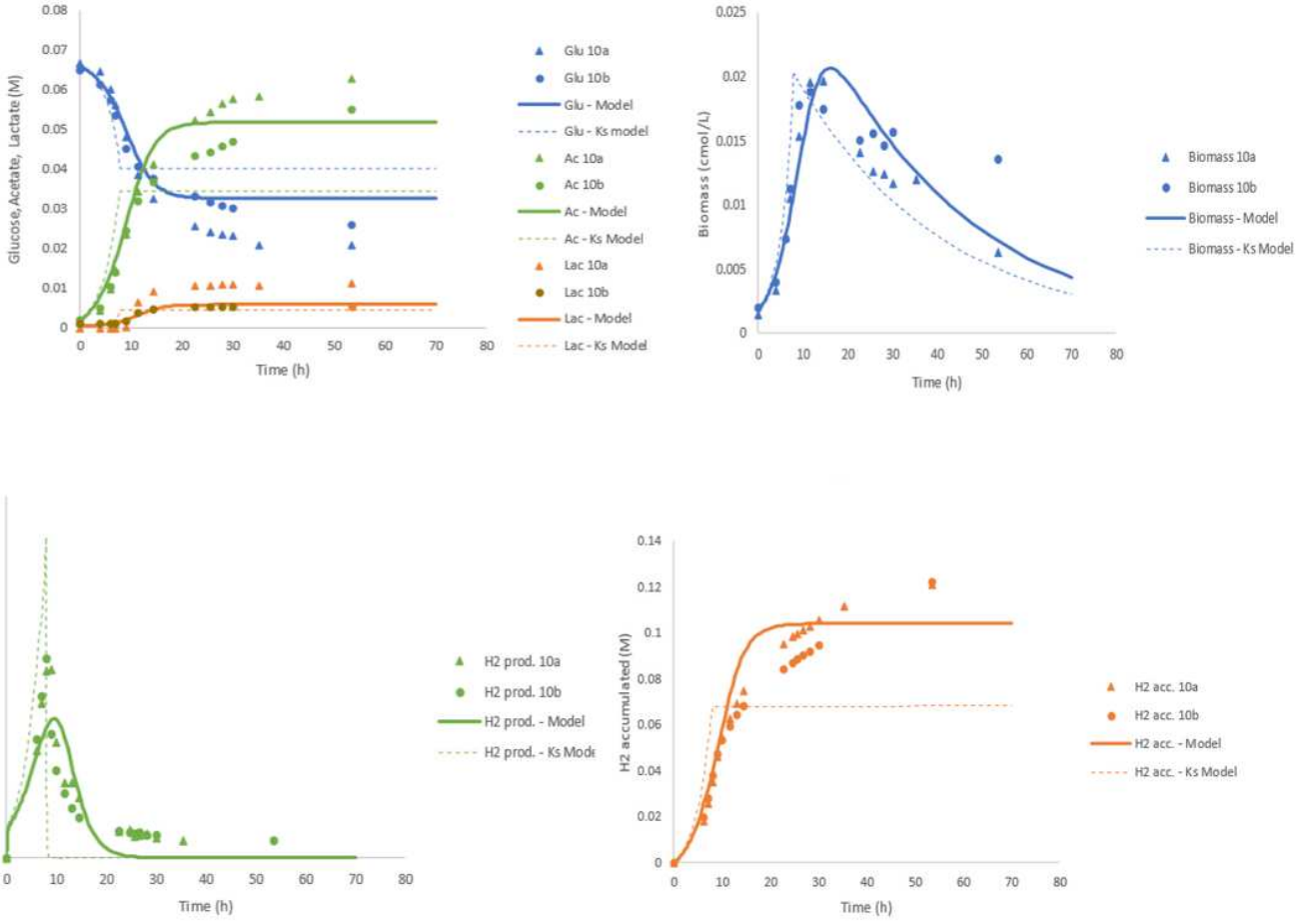

Figure 2

Experimental data (discrete points) and modelling results (lines) for the 10 g/L glucose cultures. Upper left: glucose consumption, acetate and lactate production. Upper right: biomass production. Lower left: hydrogen productivity. Lower right: accumulated hydrogen production.

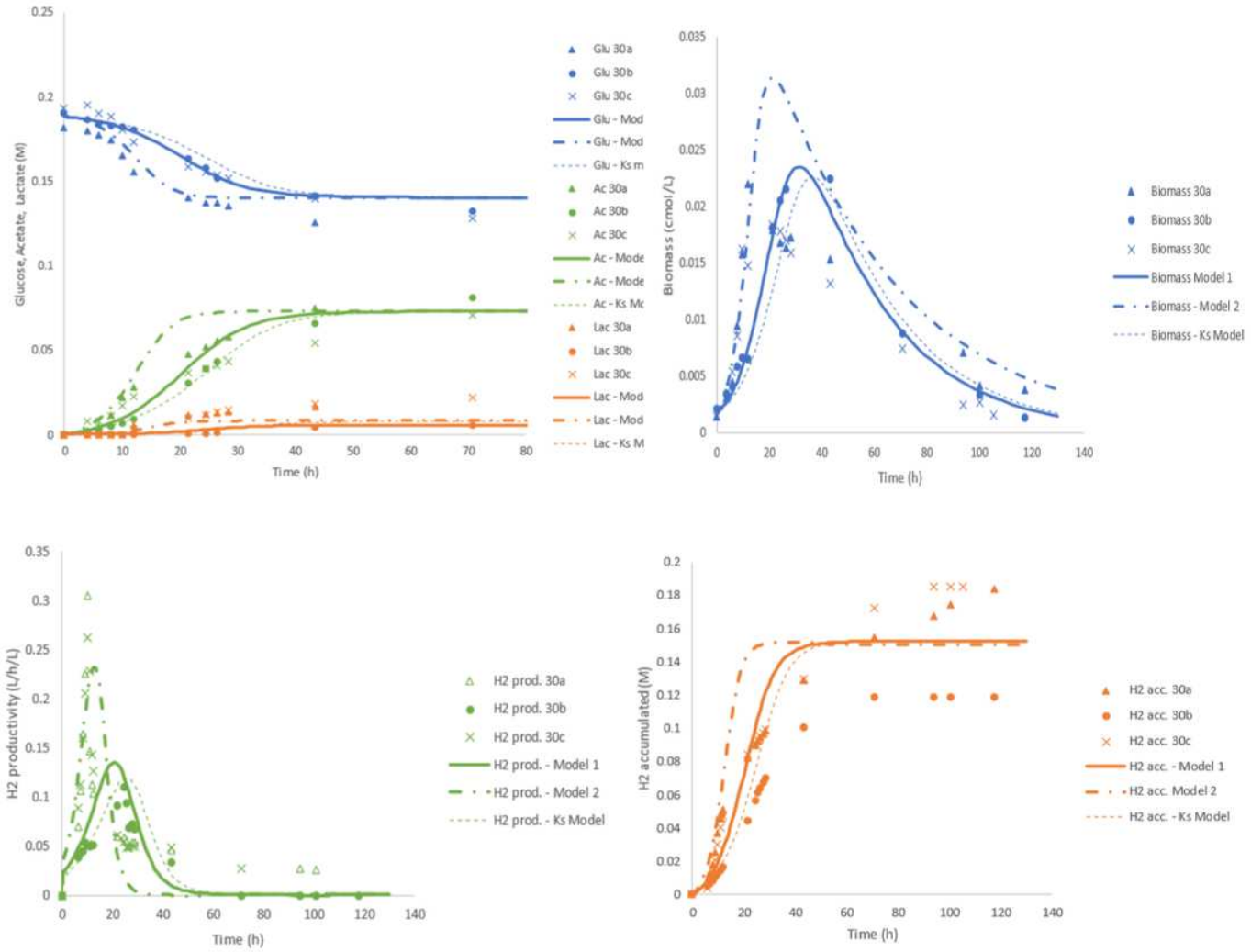

Figure 3

Experimental data (discrete points) and modelling results (lines) for the 30 g/L glucose cultures. Upper left: glucose consumption, acetate and lactate production. Upper right: biomass production. Lower left: hydrogen productivity. Lower right: accumulated hydrogen production.

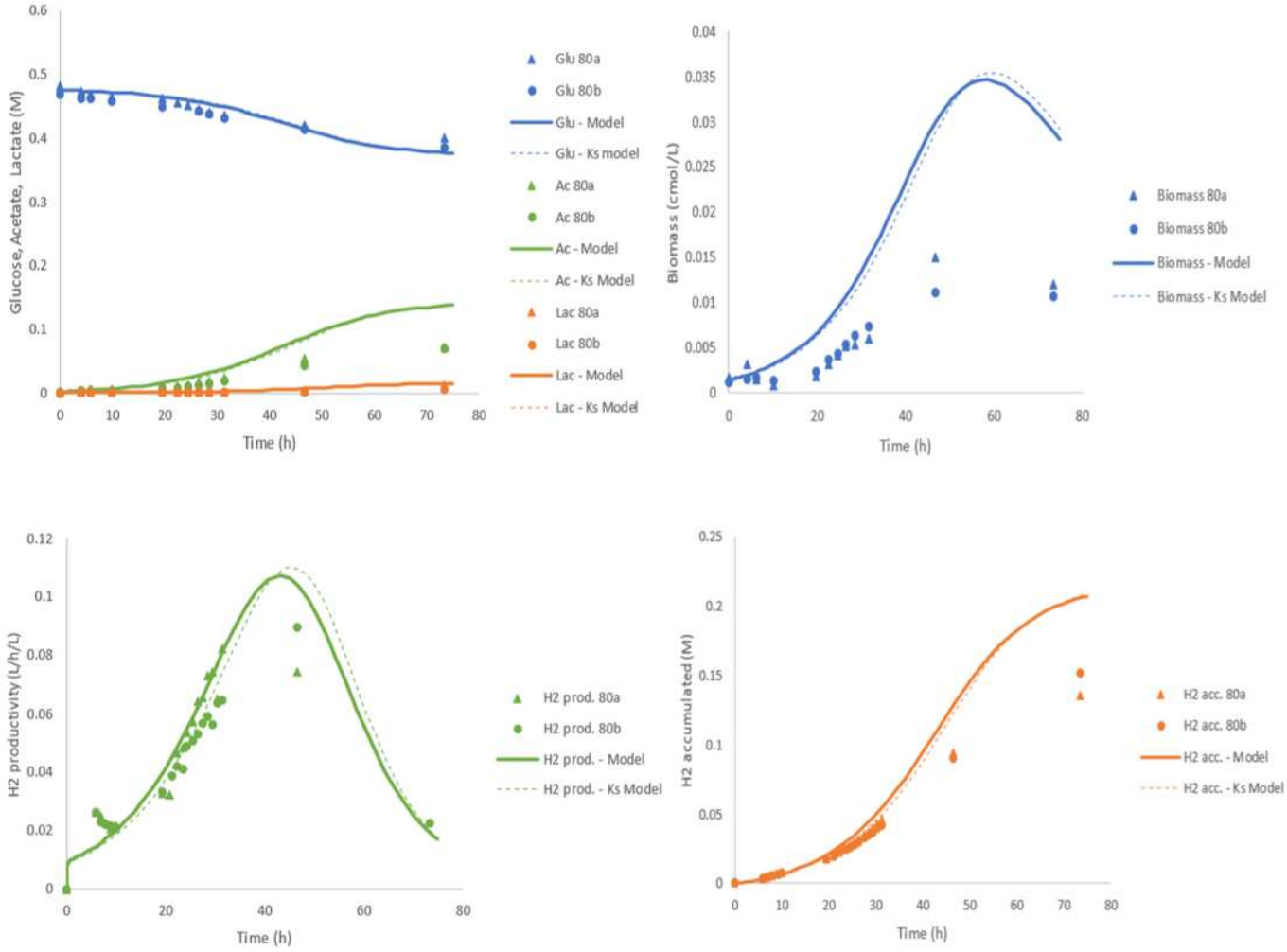

Figure 4

Experimental data (discrete points) and modelling results (lines) for the 80 g/L glucose cultures. Upper left: glucose consumption, acetate and lactate production. Upper right: biomass production. Lower left: hydrogen productivity. Lower right: accumulated hydrogen production.

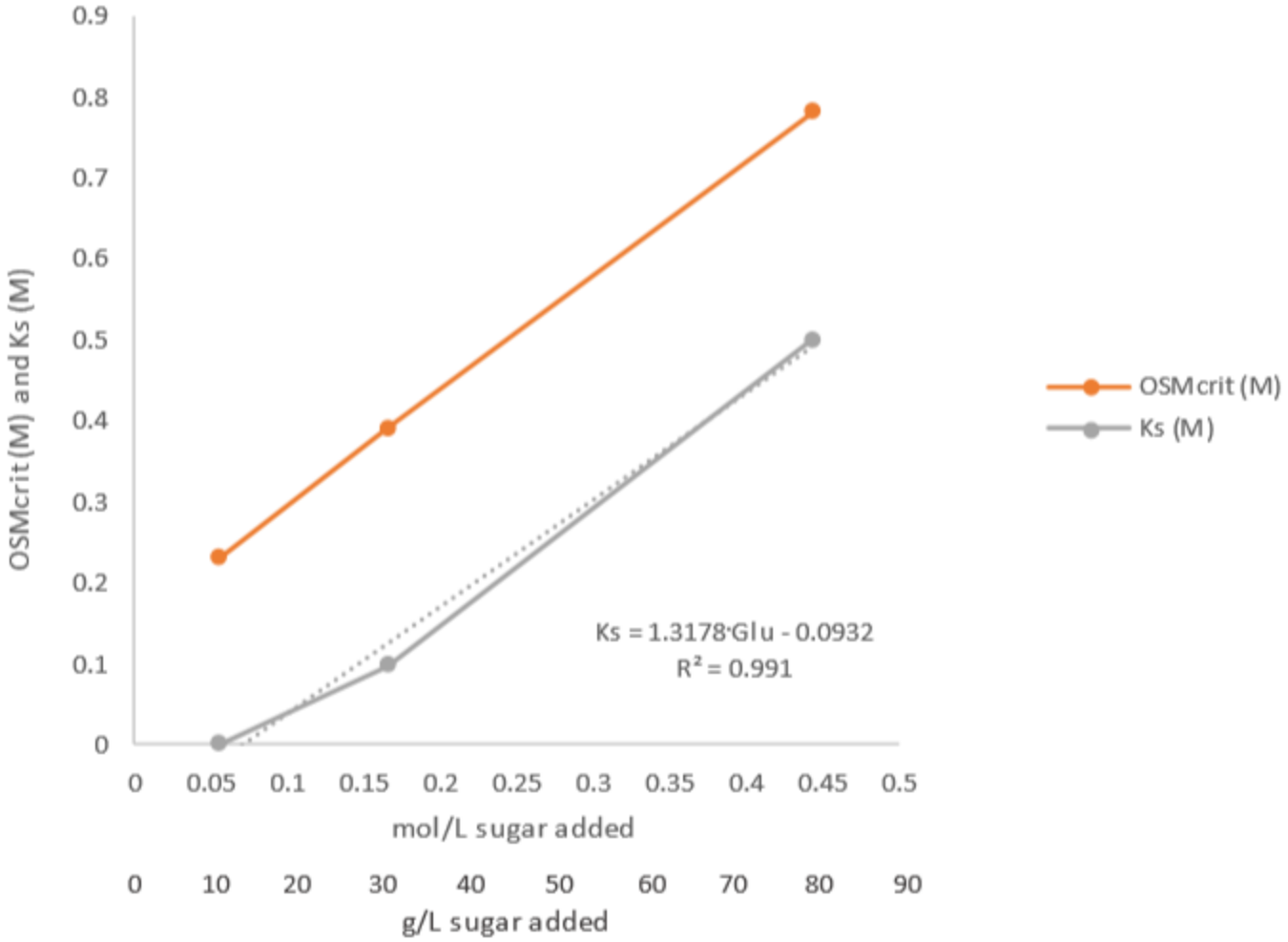

Figure 5

Comparison of the calibrated parameters OSMcrit (orange) and Ks (grey).

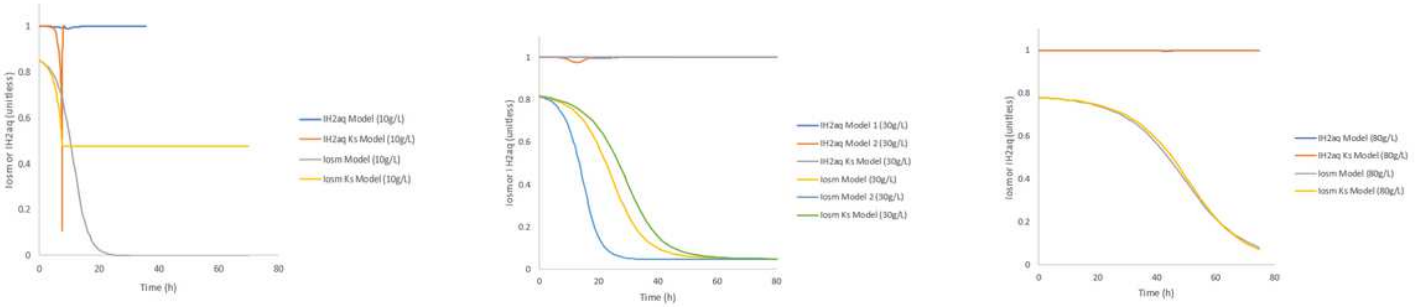

Figure 6

Simulated values of Iosm and IH2,aq for the different models